AMENDMENTS TO THE DRAWINGS

The attached two sheets of drawings are submitted as formal, replacement drawings.

REMARKS

Claims 1-10 and 12-23 are pending in the application. Claims 16-21 are withdrawn subject to a restriction requirement. No claims are presently allowed.

The paragraph beginning at page 3, line 15 has been amended to recite that the plasma can have a width of 30 cm. Support for this amendment is found in Meger et al., *Physics of Plasmas*, 8(5), 2558-2564 (2001) (page 2560, left col., lines 11-13). This publication was incorporated by reference into the instant specification at page 3, lines 17-22.

Claim 1 is amended to cancel "much" and to move the phrase that contained the term to follow "electron beam."

Claim 8 is amended to cancel an extra comma.

New claims 22 and 23 recite the ratio of width to the thickness of the electron beam. Support for the amendment is found in the paragraph beginning at page 3, line 15, as amended on 03/15/2005, where beams of 30 cm × 1 cm and 1 m × 1 cm are disclosed.

No new matter has been added.

Claim Rejections – 35 U.S.C. § 112

Claim 1 has been rejected under 35 U.S.C. § 112, second paragraph as being allegedly indefinite for failing to particularly point out and distinctly claim the subject matter which Applicants regard as the invention. The claim recited "much larger." By this amendment, "much" has been canceled.

Claim Rejections – 35 U.S.C. § 103

Claims 1-3, 7-9, and 15 have been rejected under 35 U.S.C § 103(a) as allegedly unpatentable over Meger et al. (*Physics of Plasmas*) in view of Moseson et al. (US 3,393,142).

Claim 1 is directed to a plasma deposition system, comprising an electron beam source, magnetic means, a source location, and a substrate location. The electron beam has a width larger in dimension than its thickness and is capable of sustaining an electron beam having an average electron energy of at least about 1 keV in the presence of 10 mTorr of oxygen. The magnetic means is for confining the beam so as to produce a plasma sheet. The plasma sheet is of pre-determined width, length, thickness, and location and has an electron temperature of about 1.5 eV or lower. The source location is for a material source and comprises sputtering means,

vaporization means, or both. The substrate location is for a substrate upon which material sputtered or evaporated from the source is deposited.

Moseson discloses a cathode sputtering apparatus. The apparatus includes a filament cathode and an anode held at a voltage difference of about 40 V (col. 5, line 15) to produce an electron sheet. The electron sheet produces a plasma between a target and a substrate.

In order to make a *prima facie* case of obviousness, there must be a rationale to combine the references. The Examiner stated that the motivation for utilizing the sputtering target, substrate location, and sputtering sources of Moseson is that it allows for reducing the energy requirement for sputtering operations (Answer of 12/14/2007, page 7, lines 12-15). However, the energy reduction of Moseson is realized by the electron beam generating and confining portion of the apparatus, not the sputtering portion. The Examiner's purported combination uses the electron beam generator of Meger and the sputtering apparatus of Moseson, which would show the energy reduction of Moseson.

Further, there is no motivation to combine the references because Moseson teaches the desirability of reducing the energy requirements of sputtering operations (col. 1, lines 50-52). The energy required for sputtering would be minimized when the production of plasma is optimized. Indeed, Moseson teaches the desirability of a strong plasma (col. 3, lines 56-57). It is not obvious to use the e-beam of Meger for deposition because, for example, the higher energy electrons of Meger do not have an optimized ionization cross section for a given gas. The attached Declaration Under 37 C.F.R. § 1.132 includes a graph that shows the ionization cross-sections for nitrogen as a function of electron energy. Low energy electrons, such as 40 eV in Moseson are at or near the maximum ionization cross sections in most gases and are thus very likely to collide with and ionize the gas. Increasing the energy to 1 keV decreases the ionization cross section and reduces the amount of plasma formed per length of electron travel.

A nonobvious feature of the present invention is that electron energies above 1 keV in the presence of a magnetic field produce plasma more uniformly over longer beam lengths. Higher energy electrons are more likely to go a greater distance before ionizing the gas and less likely to have non-ionizing collisions or elastic collisions. The magnetic field limits scattering via collisions with the background gas and since less energy is lost to elastic collisions, ionization and thus plasma production is more uniform over the entire length of the beam. This advantage is not limited to gas pressure or type, including reactive gases. Nothing in the references

suggests that this would be useful for sputtering or other deposition techniques. As there is no motivation to combine, a *prima facie* case of obviousness has not been made.

Further, the high energy electrons may also produce a different mix of ions and radicals (*in* molecular gases) than the low energy electrons of Moseson. For example, the attached article, Leonhardt et al., "Applications of Electron-Beam Generated Plasmas to Materials Processing," *IEEE Trans. Plasma Sci.*, 33(2), 783 (2005), shows that a high energy beam in nitrogen gas produces a high fraction of N^+ ions relative to N_2^+ ions (Fig. 2). At low energy, mostly N_2^+ ions are expected. This feature is significant in that the type of ion is as important as the amount of ions in deposition applications.

In the advisory action of 12/10/2005, the Examiner stated that it would be obvious to modify Meger with a sputtering target since Meger suggests utilizing the apparatus for other processes and that "such processes could include sputtering targets for electron beam apparatus as demonstrated by the secondary reference (Moseson)." Even if Meger suggests the use of the beam for other processes, the references do not suggest that sputtering would be such a process for the reasons explained above.

Claims 2, 3, 7-9, and 15 depend from and contain all the limitations of claim 1 and are asserted to distinguish from the reference in the same manner as claim 1.

Claims 4, 5, and 10 have been rejected under 35 U.S.C § 103(a) as allegedly unpatentable over Meger in view of Moseson and further in view of Oda et al. (US 3,436,332).

Oda discloses a sputtering apparatus using a filament cathode. The anode to cathode voltage is 60-100 V (col. 2, lines 55-56).

Claims 4, 5, and 10 depend from and contain all the limitations of claim 1 and are asserted to distinguish from the references in at least the same manner as claim 1, in that there is no motivation to combine Meger and Moseson.

Further, the Examiner stated that the motivation for biasing the substrate as in Oda is that it prevents electrons from entering the electron tube guide 16 (col. 3, lines 15-18). This statement from Oda is not understood, as there is no reference number 16 found in the drawings, so the location of the tube cannot be determined. Regardless of what the tube refers to, the bias referred to is not applied to the substrate. It is generated by power supply 24, which is applied to the filament 11, not the substrate 51.

Claims 6 and 12 have been rejected under 35 U.S.C § 103(a) as allegedly unpatentable over Meger in view of Moseson and further in view of Hurwitt et al. (US 6,416,635). Hurwitt discloses a sputtering apparatus where the target is moveable with respect to the substrate (abstract). The target is the source of both the electrons (i.e. the means to produce a plasma) and the sputtered material (col. 1, lines 13-29).

Claims 6 and 12 depend from and contain all the limitations of claim 1 and are asserted to distinguish from the references in at least the same manner as claim 1, in that there is no motivation to combine Meger and Moseson.

Claims 13 and 14 have been rejected under 35 U.S.C § 103(a) as allegedly unpatentable over Meger in view of Moseson and further in view of Bunshah et al. (US 4,336,277). Bunshah discloses a physical vapor deposition system using a filament in a very low concentration of oxygen.

Claims 13 and 14 depend from and contain all the limitations of claim 1 and are asserted to distinguish from the references in at least the same manner as claim 1, in that there is no motivation to combine Meger and Moseson.

In view of the foregoing, it is submitted that the application is now in condition for allowance.

In the event that a fee is required, please charge the fee to Deposit Account No. 50-0281, and in the event that there is a credit due, please credit Deposit Account No. 50-0281.

Respectfully submitted,

Joseph T. Grunkemeyer
Reg. No. 46,746
Phone No. 202-404-1556
Office of the Associate Counsel
(Patents), Code 1008.2
Naval Research Laboratory
4555 Overlook Ave, SW
Washington, DC 20375-5325

Applications of Electron-Beam Generated Plasmas to Materials Processing

Darrin Leonhardt, Christopher Muratore, and Scott G. Walton

***Abstract*—Nonequilibrium ($T_e \gg T_{ion,gas}$) plasma processing often allows for greater process control with reduced environmental impact when compared to other materials processing methods, and therefore presents tremendous opportunities in the areas of thin film development and surface modification. The U.S. Naval Research Laboratory's "*L*arge *A*rea *P*lasma *P*rocessing *S*ystem" (LAPPS) has been developed based on the high-energy (2 keV) electron-beam ionization process, with the goal of maximizing the benefits of plasma processing over large areas ($\sim$1 m^2). This system has been shown to be: 1) efficient at producing plasma in any gas composition; 2) capable of producing low-temperature plasma electrons ($<$0.5 eV) in high densities ($10^9 - 10^{12}$ cm^{-3}); and 3) scalable to large area (square meters).**

In this paper, the progress of a number of applications using LAPPS is discussed. Nitride growth in stainless steel was investigated, which demonstrated high rates (over 20 μm/h$^{1/2}$) at low temperatures ($\leq$462 °C). Complementary mass spectrometry showed that the nitriding results correlated to the flux of atomic ions delivered to the substrate. LAPPS was also combined with magnetron sputtering sources to form hybrid systems for thin film deposition of nitrides. The simultaneous operation of LAPPS with a titanium magnetron sputter source increased the growth of the $\langle 200 \rangle$ orientation in TiN films, due to the increased atomic nitrogen ion flux. Polymer pretreatment studies were also initiated in these systems; polytetrafluoroethylene substrates pretreated with an oxygen LAPPS exposure demonstrated a significant increase in copper and aluminum film adhesion compared to untreated substrates, with the dominant factor believed to be the changed surface morphology. Similarly dramatic fluorination of polyethylene was demonstrated with plasmas generated in Ar/SF$_6$ mixtures.

***Index Terms*—Electron-beam applications, materials processing, plasma generation, plasma materials-processing applications, surface treatment.**

I. Introduction

CONVENTIONAL plasma discharges used in surface modification applications directly heat electrons with externally applied electromagnetic fields to ionize the gas. A significant amount of input power is therefore lost to low-energy (0–10 eV) gas excitation processes, rather than ionization or dissociation processes (10–20 eV) that produce the desired reactive plasma species. Additionally, plasmas sustained by heated electrons require electron temperatures of multiple electron volts, which generally translate to a plasma environment of high plasma potentials (>10 V), sheath drops, and ion isotropy at surfaces. However, when a high energy beam of electrons passes through a gas, its dominant process is ionization of the gas followed by dissociation and finally excitation. The resultant plasmas, which are not relying on the plasma electrons to initiate ionization, have low electron temperatures and plasma potentials making them desirable for many surface modification applications. Furthermore, the direct ionization mechanism makes the plasma production process extremely efficient and the electron beam is easily scalable to large areas (square meters) when compared to conventional plasma discharges.

Fernsler *et al.* [1] and Manheimer *et al.* [2] have discussed the detailed physics behind the plasma production mechanisms from electron beams, which agree with experimental *in situ* measurements [3], [4]. More recently, a broader view of electron-beam (e-beam) generated plasmas was presented [5] to illustrate both the fundamental aspects and the range of plasma source configurations being investigated for various applications. This paper reports on the continual experimental progress of various applications with e-beam generated plasmas and their incorporation into multiple plasma source systems that are being pursued for materials' modification. These applications include the nitriding of stainless steel, surface activation of various polymer materials, and thin film deposition of metal-nitrides.

II. Experimental Methods

For all experiments discussed in this paper, a plasma "layer" was used, as discussed previously [6]. Briefly, a sheet of high-energy electrons was produced by a linear hollow cathode to generate the plasma layer. The hollow cathode was nominally driven by -2 kV, 2 ms pulses at 50% duty factors with typical e-beam currents of 0.05–0.5 mA/cm^2, depending on the application. No attempts were made to optimize the processes by varying the plasma's duty factor. The e-beam was accelerated out from the 1.0 cm wide hollow channel and skimmed by an aperture in a grounded stainless steel anode to set the geometric shape of the beam. The anode was located $\approx$5 cm in front of the cathode and contained a 1 cm wide slot of the same length as the cathode (15–25 cm). An axial 16.5 mT magnetic field provided by Helmholtz coils kept the beam profile planar. The e-beam was terminated at another stainless steel anode, which was >40 cm away from the slotted anode.

The arrangement of the plasma processing system is shown in Fig. 1. The processing stages (or substrate holder) were introduced laterally, to the "face" of the plasma layer. Stages were

Manuscript received August 31, 2004; revised October 7, 2004. This work was supported by the Office of Naval Research and the American Society for Engineering Education (ASEE). The work of C. Muratore was supported by an ASEE postdoctoral fellowship at the Naval Research Laboratory.

D. Leonhardt and S. G. Walton are with the Plasma Physics Division, U.S. Naval Research Laboratory, Washington, DC 20375 USA (e-mail: darrin@ccs.nrl.navy.mil; sgwalton@ccs.nrl.navy.mil).

C. Muratore was with the Plasma Physics Division, U.S. Naval Research Laboratory, Washington, DC 20375 USA. He is now with the Wright Patterson Air Force Base, Dayton, OH 45433 USA (e-mail: chris.muratore@wpafb.af.mil).

Digital Object Identifier 10.1109/TPS.2005.844609

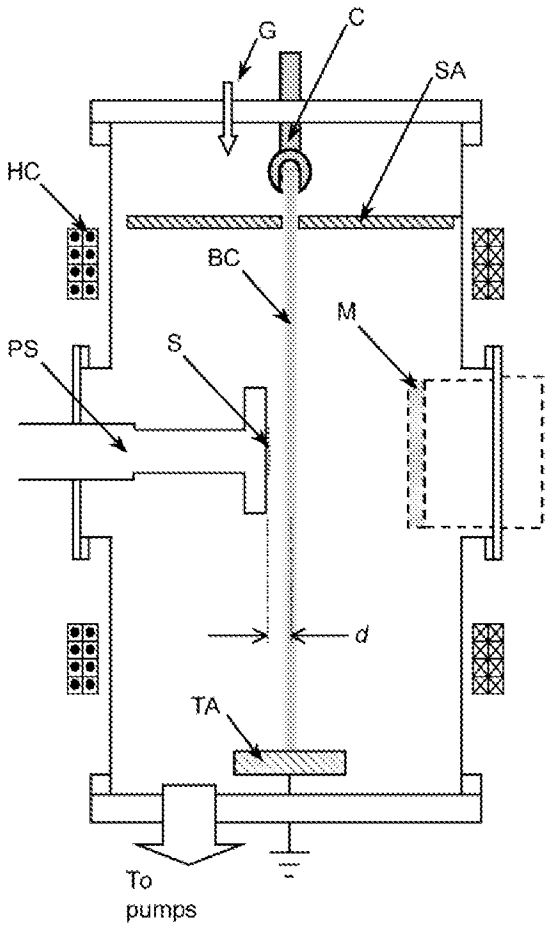

Fig. 1. Experimental arrangement for e-beam generated processing system. System components are labeled as follows: (C) cathode; (G) gas feed; (SA) slotted anode; (TA) termination anode; (HC) Helmholtz coils; (BC) e-beam channel and plasma; (S) substrate; (PS) processing stage; (M) additional magnetron source; and (d) distance from beam center to substrate surface.

constructed with grounded support structures, temperature control capabilities, and an electrically isolated electrode 11 cm in diameter that was recessed in a ceramic insulator. When magnetron sources were incorporated, they were located opposite the stage on the other side of the e-beam produced plasma and were not modulated (100% duty factors). Samples were ultrasonically cleaned in acetone and/or methanol then dried prior to being mounted in the vacuum chamber, typically 1.5 cm from the center of the beam channel.

Experiments were carried out in a variety of vacuum chambers. Mass flow controllers were used for stable gas flow of 20–50 sccm, except in the nitriding experiments where a manual leak valve was used for nitrogen flows >50 sccm. The high vacuum pump (turbomolecular or diffusion) was throttled with a manual valve or iris to set the system's operating pressure. All chambers were metal in construction and had base pressures below 2×10^{-6} Pa.

A. Plasma Nitriding

Details of these experiments are given elsewhere [7], [8] so only minimal detail will be given here. Samples approximately 5 cm^2 were cut from a 6-mm-thick plate of 316 stainless steel and polished to a surface roughness of 0.020 μm. The e-beam generated plasma and −350 Vdc sample bias was initiated in 21.3 Pa (160 mtorr) of nitrogen and argon (88% and 12%, respectively, by partial pressure), as the sample process temperature (325–462 °C) was reached in 30 min. An internal thermocouple mounted in the stage head was calibrated against a thermocouple mounted to the surface of a sacrificial sample as it underwent various conditions of the nitriding process. The reported temperatures are, therefore, considered an accurate representation of the surface temperature. The processing stage temperature was then kept constant for an additional 6.5 h of laboratory time. After plasma exposure, the samples were allowed to cool in a nitrogen atmosphere then removed from vacuum, sectioned, and sputter coated with titanium. The sections were then polished to 1 μm, etched in Marble's solution, polished again, and analyzed with a high-resolution optical microscope (from a Vickers' microindenter) to determine the nitride layer thickness. Surface hardness was determined with an UMIS 2000 fitted with a diamond indenter.

To characterize the ion flux to the substrate, the same operating conditions were set in a system where the ion species' energy and mass could be resolved with a differentially pumped EQP300 Plasma Probe (Hiden Analytical Ltd.), as discussed in [4]. Briefly, the EQP300 is a tandem electrostatic energy analyzer/quadrupole mass spectrometer that samples plasma species through a 20 μm orifice, allowing the spectrometer to operate under high vacuum conditions. This spectrometer was magnetically shielded and gated to sample plasma species only during the e-beam pulse. The major differences between these measurements and the nitriding conditions were that a different vacuum chamber was used (base pressure below 1×10^{-6} Pa) and the sampling stage was smaller in diameter (5.7 cm) than the processing stage. Also, this stage was not actively heated and electrically grounded. In order to obtain ion energy distributions due to a direct current (dc) bias at the EQP electrode, the termination anode was biased to +100 Vdc to raise the plasma potential and thereby provide a comparable sheath drop at the grounded EQP stage. (The 100 Vdc level was used instead of the 350 Vdc level used in nitriding experiments to avoid spurious dc breakdowns around the noninsulated termination anode.)

B. Polymer Pretreatment

Two different chemical systems were used to determine the effectiveness of the e-beam generated plasma in pretreating polymer substrates. The two systems studied were chosen to increase: 1) the adhesion of metals to polymer substrates, and 2) the chemical reactivity of inert polymer surfaces. In these preliminary experiments, the conditions were not optimized for a specific outcome but to determine the effects of the surface under general conditions. For metal adhesion ("metallization") experiments, two plasma systems were operated independently; the e-beam produced plasma for surface pretreatment followed by the PVD (sputter deposition) of the metal film. Thin (70 μm) polytetrafluoroethylene (PTFE) pieces roughly 4 cm^2 were masked with 5 mm wide Kapton tape and mounted to the grounded processing stage. A sputter magnetron source with a 3 cm diameter aluminum or copper target was located 13 cm from the PTFE substrate. The relative position of the beam,

magnetron target and substrate were independently set but not optimized. Plasma pretreatment consisted of operating the e-beam at a 20% duty factor in 6.7 Pa (50 mtorr) oxygen for 10 min of exposure time (over 50 min of elapsed lab time). After plasma pretreatment, the magnetron was operated in 2.4 Pa (18 mtorr) argon at 100 W to deposit ≈700 nm thick metal films. Comparisons between the metal film adhesion with and without plasma pretreatment were carried out through visual inspection and the Association of Industrial Metallizers, Coaters and Laminators (AIMCAL) "Scotch Tape Test" [9] to qualitatively test film adhesion. To examine the effects of oxygen plasma pretreatment on the substrate material alone, water droplet contact angle goniometer (Ramé–Hart Model 100-00) measurements were used to compare the surfaces of nonmetallized treated and untreated PTFE samples. For the experiments to modify the surface chemical reactivity of inert polymers, samples of high-density polyethylene (HDPE) were exposed to e-beam generated plasmas containing sulfur hexafluoride (SF_6). Similarly sized (4 cm^2) substrates were cut from bulk (250 μm thick) HDPE, and again mounted 1.5 cm from the e-beam center. The plasma pretreatment consisted of operating the e-beam at a 20% duty factor in a 8.5 Pa (64 mtorr) mixture of argon and SF_6 (35 sccm Ar : 15 sccm SF_6) for 10 min of exposure time. The samples were removed from the plasma chamber in air and analyzed by X-ray photoelectron spectroscopy (XPS).

C. Titanium Nitride Deposition

A 15 cm diameter magnetron with a titanium target was mounted 7 cm from the processing stage to deposit thin films of titanium nitride (TiN) in an argon/nitrogen atmosphere. Silicon ⟨100⟩ substrates 2–3 cm^2 in size were cleaned by an e-beam generated plasma in 6.0 Pa (45 mtorr) argon with a −50 Vdc bias on the stage, while heated to 250 °C over the course of 15 min. The temperature was stabilized an additional 3 min, then the magnetron target was powered to 800 W. After 2 min of operation in pure argon, 0.9 sccm of nitrogen was added, resulting in no change of process pressure. Nitride deposition was then carried out with both plasma sources for 20 min with the substrate maintained at 250 °C and −50 Vdc. For comparison, films were grown with only the magnetron source for the same deposition time, keeping the average ion current to the sample stage the same as measured in the hybrid system (0.6 mA/cm^2) by minor (<2%) adjustments in the externally applied axial magnetic field. X-ray diffraction (XRD) and atomic force microscopy (Digital Instruments AFM) were used to characterize the resultant TiN films.

III. Results and Discussion

A. Plasma Nitriding

Table I shows the sample temperature and resultant nitride layer thickness as determined by the microscope measurements. The nitrided layer thickness and plasma exposure time (50% of 7.0 h) were used to calculate nitriding rates at various temperatures for the process, assuming a diffusion-controlled growth rate mechanism [10], [11]. This diffusion-controlled growth rate is proportional to the square of the layer thickness

TABLE I
Measured Nitride Layer Thickness at Various Substrate Temperatures; Plasma Operation and Conditions Are Given in Text

TEMPERATURE (°C)	NITRIDE THICKNESS (microns)
462	40.0
445	21.7
415	12.2
355	4.7
325	2.2

divided by the growth time, or $d^2/t \equiv D_0 \exp(-E_a/\mathrm{kT})$ where d is the nitride layer thickness, t is the exposure time, E_a is the effective activation energy for diffusion, and T is the temperature. A linear least squares fit of the natural logarithm of the rates versus temperature (i.e., Arrhenius plot) gave an activation energy of 101.5 kJ/mol (1.4 eV/atom) for this process. Each sample's hardness was also measured to be ≈ 15.5 GPa throughout the nitride layer, compared to the untreated stainless steel surface of 2.6 GPa. The nitriding results of these experiments with little optimization are comparable with those in the recent literature [12], [13] and considerably faster than standard techniques using radio frequency (RF) and dc glow discharges (see [7] and the references therein). The observed low activation energy for this process is highly desirable, as it results from a more thermodynamically favorable chemical environment for plasma nitriding. Furthermore, by nitriding the surface of stainless steel at these low temperatures (≤462 °C), the intrinsic corrosion-resistant properties of the stainless steel are preserved while the surface becomes much harder due to the nitride layer.

The composition of the ion flux measured with the EQP300 at various distances from the e-beam showed (Fig. 2) comparable amounts of molecular and atomic nitrogen ions up to 3 cm from the e-beam center. The flux dependence in Fig. 2 illustrates the fundamental difference between the present e-beam plasma nitriding experiments and other plasma nitriding systems: e-beam generated plasmas produce a large relative flux of atomic nitrogen ions and low electron temperatures. The abundance of cold plasma electrons in this system can rapidly recombine with the molecular ions outside the ionization region (beam channel) and, thereby, reduce the N_2^+ flux to the substrate. This causes the flux of the two nitrogen ion species to become comparable, unlike other nitriding systems where high-plasma electron temperatures allow only the flux of the less chemically reactive molecular ions to dominate. The corresponding nitriding rates normalized to the measured ion currents at various substrate locations and fixed temperature (415 °C) are given in Fig. 3. The nitriding rate demonstrated a highly nonlinear dependence with distance, or the monotonically decreasing ion current (top axis in Fig. 3).

Fig. 4 shows the normalized ion energy distribution functions (IEDFs) acquired during the e-beam operation for the dominant

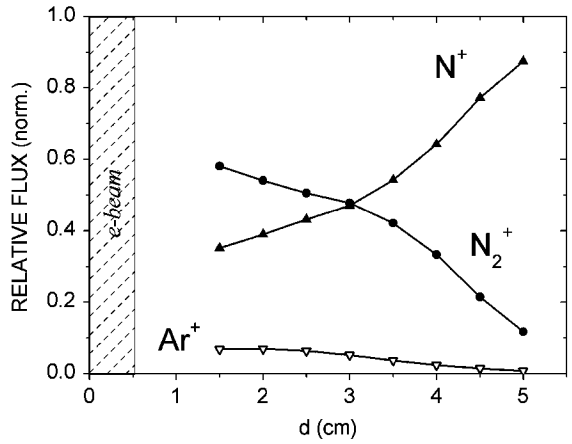

Fig. 2. Normalized ion flux measured with the EQP300 at various distances from the e-beam for the plasma conditions of 21.3 Pa total pressure (88% N_2/12% Ar by partial pressure), 50% plasma duty cycle, and a grounded sampling stage.

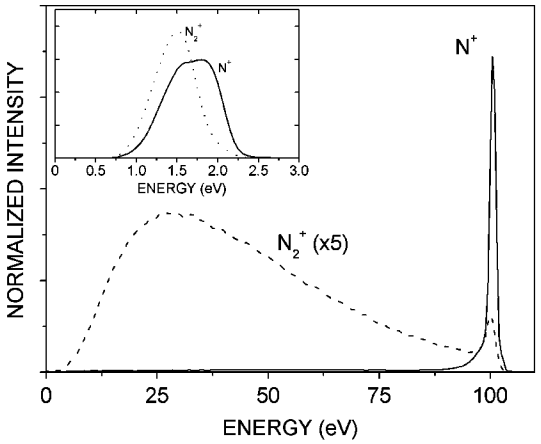

Fig. 4. Ion energy distributions of nitrogen species traversing an imposed 100-V sheath and with typical e-beam generated plasma sheath (inset) at the same conditions used in Fig. 2.

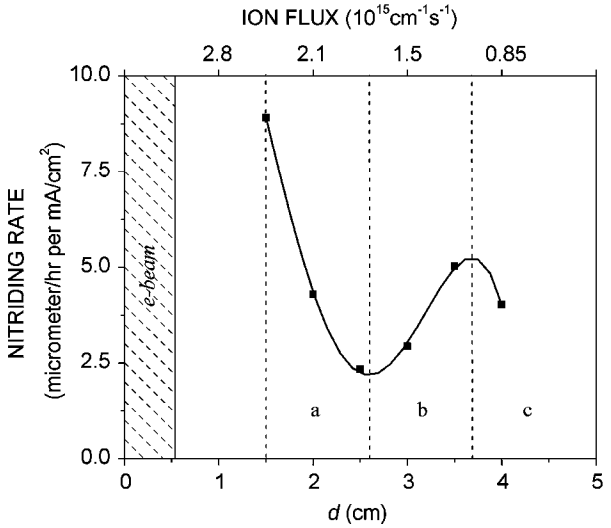

Fig. 3. Stainless steel nitriding rate normalized to ion current at various distances from the e-beam. Conditions are the same as in Fig. 2, but the substrate was 415 °C and biased at −350 Vdc.

molecular and atomic ion fluxes with a 100-V sheath drop. For comparison, the insert shows the IEDFs with no external biasing (note that 1 eV $= 1.6602 \times 10^{-19}$ J). With no external bias (inset), both ions showed narrow (<1 eV full-width at half-maximum) low energy (0.8–2.5 eV) distributions. The applied bias of 100 V shifted the atomic IEDF to approximately 100 eV, but the molecular ion showed a broad distribution spanning the entire energy range, with a most probable energy of 25 eV and a small secondary peak in energy at 100 eV. This data showed that the atomic ions arrive at the surface with the full sheath voltage unlike the molecular ions, which lose a significant portion of their acquired sheath-drop energy to charge exchange collisions [14] within the sheath. (The charge exchange cross section for N_2 is $\sim 10^{-15}$ cm^2 resulting in a mean free path comparable to the sheath thickness of ~1 mm at these pressures, whereas the momentum change cross section for atomic nitrogen in molecular gas is an order of magnitude less.) The atomic ion was therefore considered critical in the formation of the nitrided layer because: 1) the increased energy delivered to the substrate surface, and 2) it is atomic nitrogen that adsorbs and diffuses into the bulk to promote the nitride layer growth. Furthermore, at the −350 Vdc bias applied in the nitriding experiments, it is likely that only the atomic ions were capable of sputtering unwanted oxides that inhibit the nitride layer growth, given the energy loss of the molecular ions.

The normalized nitriding rates shown in Fig. 3 can now be better understood. With the substrate close to the plasma source (Region a), the ion fluxes are roughly equal and large. The rate decrease from 1.5 to 2.5 cm is monotonic with the decrease in ion current. Further from the plasma source (Region b) the molecular ion flux has decreased significantly due to electron-ion recombination while the atomic ion flux remains comparable. However, the neutral atomic flux increases proportionally with the molecular ion loss, since electron–ion recombination is dissociative. Thus, in Region 2, there was sufficient reactive neutral atomic flux to increase the normalized nitriding rate although the total ion flux had decreased, since it is only the atomic ions that carry the full sheath voltage to promote subsurface diffusion and sputter away the unwanted oxides. In Region c, the ion flux becomes too low to compete with the surface oxidation, which is occurring at one monolayer per second given the system base pressure, and nitriding diminishes rapidly.

B. Polymer Pretreatment

Results of the AIMCAL Scotch Tape tests on the metallized PTFE substrates are shown in Fig. 5, where the sample edges closest to one another (circled) were the specific areas where the test was carried out. The Kapton masking strips were removed prior to the test, leaving a striped pattern of metal and untreated PTFE. The top samples, which did not undergo any plasma pretreatment, showed a weak adhesion of the metal films: the lowest strip of aluminum has been nearly completely removed and the copper film showed only slightly better adhesion. The metal films deposited on the pretreated samples (bottom) demonstrated no peeling or separation from the substrate. The nonmetallized treated PTFE samples also showed a higher

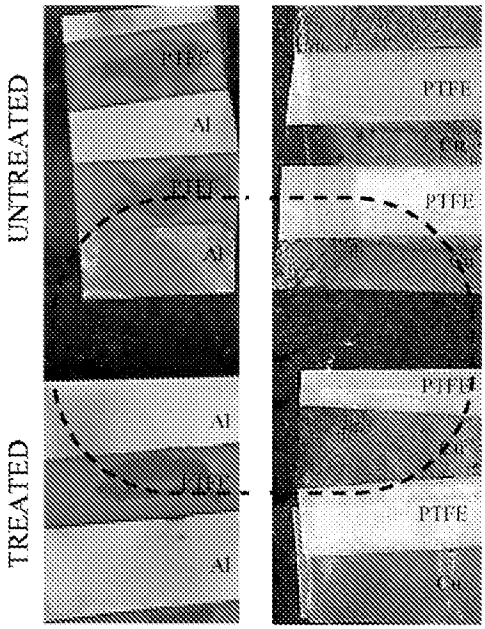

Fig. 5. Scotch Tape test areas (circled) showing removal of metal films from PTFE (top) and improved adhesion when treated by the O_2 based e-beam generated plasma (bottom). Substrates were masked with 5-mm-wide Kapton tape strips, sputter-coated with metal, and then had the mask removed before subjected to the test. Masked areas are labeled by "PTFE" while the metallized areas are labeled by "Al" or "Cu." The bottom sample was exposed to an e-beam generated O_2 plasma (6.7 Pa) for 10-min exposure time (grounded, room temperature substrate) before metallization.

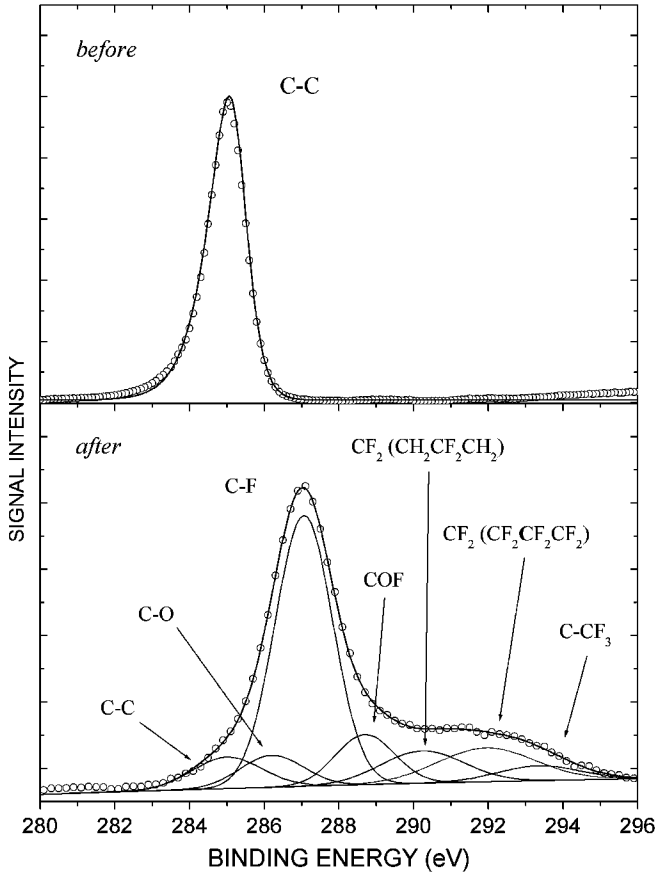

Fig. 6. XPS spectra for treated (bottom) and untreated (top) polyethylene. Treatment was with an e-beam generated 8.5 Pa Ar/SF_6 plasma (35:15 by flow, respectively) for 10 min of exposure time (grounded, room-temperature substrate).

water contact angle ($129.8 \pm 0.8°$) than the untreated samples ($119.7 \pm 0.8°$).

Although the results in Fig. 5 are quite clear, the tape tests only provide a lower bound on the adhesion performance; Chen *et al.*, [15] determined the peel strength of materials passing the test to be at least 10 kg/m. The accepted peel strength for the electronics packaging industry is 40 kg/m, therefore, more advanced peel-test measurements are necessary to qualitatively determine the improvement and practicality of the present metal adhesion. Regardless, the observed increase in metal film adhesion may be attributed to both chemical and/or physical changes of the surface. Roughening the surface by simple sputtering results in a dramatic increase in surface area and perhaps more importantly, a varying surface normal that requires additional force to remove the metal film [15], [16]. Chemically, however, such plasma pretreatments are responsible for creating a broad variety of oxygen-containing groups on polymer surfaces, which are known to increase the adhesion of metals through the large metal–oxide bond strengths. The contact angle measurements imply a less polar surface resulted from plasma treatment since water was repelled, which would indeed result if the more electronegative fluorine atoms were replaced by less electronegative oxygen atoms. However, these observations contrast earlier studies on oxygen plasma treatments of PTFE [17], [18] that showed a decrease in the water contact angle (i.e., increased wettability). Since negligible oxygen species were incorporated into the PTFE surface (by XPS) in those works, it was concluded that the decrease in contact angle was due to physical sputtering and roughening of the surface. More recent studies showed a roughened surface morphology ($r_{\mathrm{rms}} \geq 300$ nm) may also increase the water repellency of a surface [19]. In fact, contact angles $>150°$ were seen for oxygen plasma treatments over 60 s, with minimal changes in surface composition (by XPS). At longer processing times, the fast etching processes dominate the very slight chemical modification of the surface. Thus, given the extensive processing times in the present e-beam generated plasma experiments and considering that copper is a relatively inert material compared to aluminum, the improved adhesion observed in these experiments was likely to be due to the changed (physical) surface morphology rather than surface chemistry. The effects of ozone and ultraviolet (UV) light in this system were considered negligible. Ozone production in these e-beam generated oxygen plasmas was minimal due to the low-electron temperature and overall low gas density. The critical ozone precursors (negative atomic and molecular ions [20]) are not created in these plasmas [21] because of the high threshold for electron attachment at low pressures. Although, PTFE was chosen for these experiments because of its well-known resilience to UV light and ozone, more analytical surface analyzes are necessary to completely separate all of the possible chemical effects.

XPS analysis was carried out on the SF_6-treated and untreated HDPE and are compared in Fig. 6. The individual bond peaks are shown under the fitted spectra, which agreed well with the recorded data. The plasma treated substrate demonstrated a

tremendous amount of surface fluorination as the predominant aliphatic chain (C–C bond) peak became dominated by fluorinated carbon species (C–F bonds and fluorinated chains). (The fitted peaks were not exclusive solutions to the fitted spectrum, but the relative intensities were considered reasonable given the limited data.) From these spectra, it can be concluded that: 1) the unsaturated polymer groups are effectively saturated by fluorine addition [22], and 2) the polymer backbone had not been disrupted, since the fluorocarbon chains are now visible in the XPS spectra. Although argon was a significant gas constituent, the UV plasma emission [23] also did not appear to cross-link or disrupt the polymer backbone. The treated HDPE surface had become highly reactive and susceptible to further chemical modifications, an area of present study in our laboratory, as well as the aging effects of the fluorination treatment.

These tests were conducted to demonstrate the nondestructive nature of the e-beam generated plasma source (due to the low energy ions and electrons) on more delicate substrates while still producing a viable plasma (pre)treatment process. It is important to note that the excessive processing times showed no overtly deleterious effects to the surface while significantly modifying it.

C. Titanium Nitride Deposition

Resultant TiN films were ≈150 nm thick and consisted of (002) and (111) TiN crystals as determined by XRD. The films deposited with the e-beam generated plasma showed an increase in the relative amount of (002) crystals from 20% to 27% of the total composition. Assuming that the neutral titanium fluxes from the magnetron and the total ion current to the substrate were held constant, the reactive neutral and charged nitrogen species were the variable quantities between the two plasma systems used in the TiN deposition experiments. As discussed in Section III-A, the e-beam generated plasmas provide comparable atomic and molecular ion fluxes to the substrate. Also, the low-energy plasma electrons from the e-beam generated plasma are free to recombine with the molecular ions generated by the magnetron source to create an additional source of neutral nitrogen atoms. Although limited, these experimental observations agree with previous surface kinetic arguments [24], [25], which showed that an increase in atomic nitrogen flux promoted the growth of (002) grains over (111) grains. The AFM peaks in Fig. 7 similarly illustrated a lower average grain height for the film grown with the e-beam produced plasma present, consistent with the increased number density of shorter, broader islands of the (002) grains. Therefore, a consistent correlation was seen between the (002) TiN film growth and the additional nitrogen fluxes provided by the e-beam produced plasma system.

D. E-Beam and Plasma Operation

For the 0.05–0.5 mA/cm^2 e-beam currents, the hollow cathode operating current was roughly and order of magnitude greater and, therefore, utilized powers ranging from 15 to 250 W, as calculated from the product of the current densities, cathode hollow active areas (15–25 cm by 1 cm), and the applied operating voltage (2 kV). Very little power is distributed

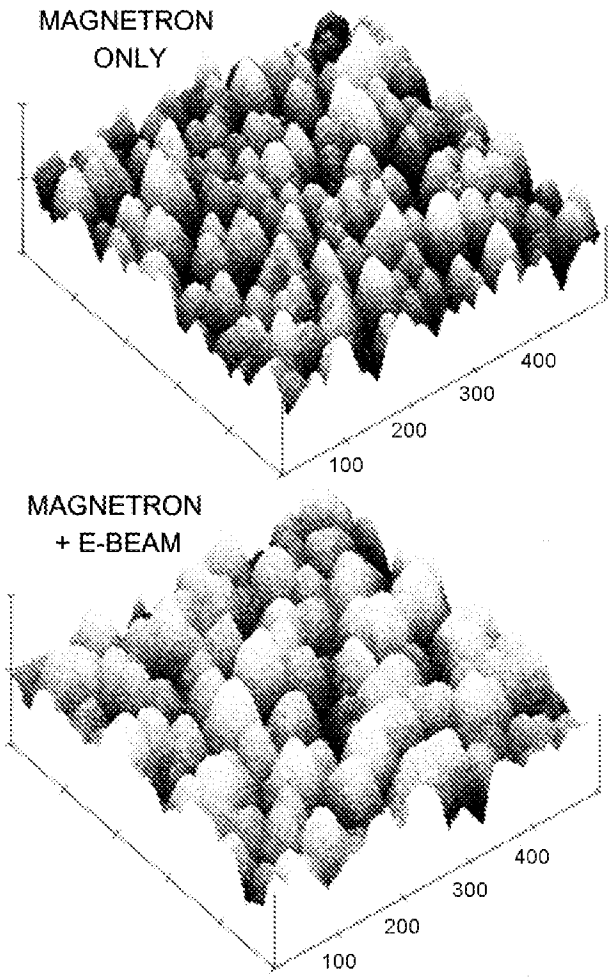

Fig. 7. AFM data for TiN grown films in the magnetron + e-beam produced plasma system (bottom) showing a significantly lower average grain height and an increased number density of shorter, broader islands than the magnetron-only (top) system. Both systems were operated at 6.0 Pa of Ar/N_2 (25:0.9 by flow, respectively) with the substrate stage heated to 250 °C and biased −50 Vdc.

in the chamber from the e-beam (1.5–25 W) or plasma generated by the e-beam (see [1] for the complete analytic theory). More efficient e-beam production (beam current >80% of source current) has been demonstrated in our laboratory [26] and others [27], which can in turn significantly reduce the required input (cathode) power. In many instances however, the largest power consumption comes from the generation of the 16.5 mT magnetic field with electromagnets to collimate the e-beam, which required ≈100 W for the Helmholtz coils (≈ 55 A × 20 V) used in these experiments. If the magnetic field power could be reduced or removed, with permanent magnets for instance, this power consumption could also be decreased dramatically. Considering the largest area (25 cm × 40 cm) e-beam used in this work, each side of the plasma sheet has two 500 cm^2 active areas for materials processing, or 1000 cm^2 total active area, for ≈ 350 W. Even with these nonoptimum designs, no other plasma processing system can provide such large processing areas from such minimal power.

Now consider the propagation of the e-beam in the processing chamber. At the energies and pressures used in these

experiments, an e-beam loses ~0.15% of its energy per centimeter of propagation ($dE_b/dz \sim N \ln(E_b)/E_b$; see [28]) and the range for an e-beam propagating in a background gas varies as $E_b^2/(N \ln(E_b))$, where E_b is the beam energy and N is the gas density. Thus, for a cathode operating at 2 kV, the e-beam can travel 1.8 m in 6.6 Pa (50 mtorr) of molecular oxygen. This effective beam range was much longer than the systems used here to ensure uniform beam energy and therefore, ionization rates along the length of the beam in the system. (It should be pointed out here that for the previous discussion on operational power, the beam range could easily be doubled without loss of uniformity, thereby doubling the effective active area of the plasmas used in these experiments.) At these low e-beam currents, dumping the partial or the full beam current to either anode did not show any ill-effects to the processing system in terms of sputtered material or system contamination [29], although high beam energies ($\gg$1 mA/cm^2, 4 kV) have been observed to rapidly heat the impact areas of the anodes [30] to a dull glow. The plasma generation by the e-beam is straightforward although not necessarily as intuitive as stated earlier. (For a complete analytic treatment of the following discussion, see [1] and [2]). From the discussion above, on average the majority of the e-beam energy is dumped into the termination anode and very little energy is deposited in the gas. The majority of the e-beam interactions with the gas result in ionization (regardless of composition) with low energy secondary electrons. Statistically, the e-beam may give up to one-half of its energy to the secondary electron in a collision with a gas molecule, which results in the secondary electron effectively becoming part of the high-energy beam. Secondary electrons generated with lower energies (say 0–10% of the beam energy) rapidly give up their energy to the gas through elastic and inelastic collisions (depending on the dominant collision cross sections), further ionizing, dissociating, and finally exciting the background gas. At the pressures typically used, this cooling process takes a few microseconds. This is the fundamental difference in e-beam generated plasmas versus conventional discharges: plasma electrons created by an e-beam quickly cool to the threshold of the lowest inelastic process (typically a vibrational excitation <0.5 eV) of the gas, whereas conventional discharges (capacitive, inductive, dc/RF glows, electron-cyclotron resonance) need to continually reheat the plasma electrons to a few electron volts in order to maintain the desired ionization rate.

IV. Summary and Conclusion

Electron-beam generated plasmas were used in various surface modification applications. Their primary advantages for materials applications are: 1) low-temperature plasma electrons; 2) operational independence from plasma gas composition; and 3) plasma production efficiency and inherent scalability. These plasma sources demonstrated considerable flexibility for modifying materials alone and when coupled with sputter magnetron sources. When used alone, the absence of high plasma electron temperatures (and, therefore, large plasma potentials) allows a variety of processing conditions without sacrificing flux of reactive charged or neutral species. This work demonstrated the important attributes of ion energy control and ion flux composition in plasma processing environment.

As discussed previously in the literature, e-beam generated plasmas are quite different than conventional discharges. The fact that e-beam produced plasmas in diatomic gases can supply predominantly atomic [4] ions to the workpiece makes it an attractive system for plasma nitriding of materials. Competitive stainless steel nitriding rates (up to 20 μm/h$^{1/2}$) were obtained below 462 °C by providing a significantly higher flux of atomic nitrogen ions from the plasma in a pure nitrogen background. These rates were accompanied by a low process activation energy of 101.5 kJ/mole (1.4 eV/atom) at modest ion energies (350 eV). At these processing conditions, the high corrosion resistance of the bulk stainless steel was preserved with an increased final surface hardness of the nitride (15.5 GPa).

In polymer applications, e-beam generated plasma treatments improved the adhesion of aluminum and copper films on PTFE and increased the chemical reactivity of HDPE, with no noticeable negative effects. Modification of the PTFE surface morphology was directly observed after oxygen plasma treatment and was considered the dominant factor in the increased film adhesion, determined to be >10 kg/m from a standard tape test. The fluorination of polyethylene with Ar/SF_6 plasmas demonstrated tremendous surface reactivity changes as fluorocarbon bonds appeared throughout the XPS spectrum. However, additional process optimization and surface analyzes that are chemically sensitive are necessary to quantitatively determine the roles of the various mechanisms in these experiments.

The incorporation of an e-beam plasma source during reactive sputtering of TiN revealed that film microstructure could be controlled by the ion flux composition, with an increased atomic nitrogen flux corresponding to an increase in (002) orientation for TiN. The preferential growth of the (002) orientation also resulted in broader features in the films, as seen and predicted by others.

The present experiments were detailed proof-of-concept tests for the practicality of applying e-beam generated plasmas in materials applications. The versatility of modulated plasmas in process space offers advantages not always accessible with continuous plasma sources, an area yet to be explored in these systems to further optimize processes.

Acknowledgment

C. Muratore would like to acknowledge the support of the American Society of Engineering Education. The authors are grateful to Dr. I. L. Singer and Dr. A. Piqué of NRL for access to materials characterization equipment and encouraging conversations, as well as Dr. V. Shamamian and Dr. D. Guerin, formerly of NRL, for their expertise with the XPS data.

References

[1] R. F. Fernsler, W. M. Manheimer, R. A. Meger, J. Mathew, D. P. Murphy, R. E. Pechacek, and J. A. Gregor, "Production of large-area plasmas by electron beams," *Phys. Plasmas*, vol. 5, pp. 2137–2143, May 1998.

[2] W. M. Manheimer, R. F. Fernsler, M. Lampe, and R. A. Meger, "Theoretical overview of the large-area plasma processing system (LAPPS)," *Plasma Sources Sci. Technol.*, vol. 9, pp. 370–386, 2000.

[3] D. Leonhardt, S. G. Walton, D. D. Blackwell, W. E. Amatucci, D. P. Murphy, R. F. Fernsler, and R. A. Meger, "Plasma diagnostics in large area plasma processing system," *J. Vac. Sci. Technol. A, Vac. Surf. Films*, vol. 19, pp. 1367–1373, Jul. 2001.

[4] S. G. Walton, D. Leonhardt, D. D. Blackwell, D. P. Murphy, R. F. Fernsler, and R. A. Meger, "Ion energy distributions in a pulsed, electron beam-generated plasma," *J. Vac. Sci. Technol. A, Vac. Surf. Films*, vol. 19, pp. 1325–1329, Jul. 2001.

[5] D. Leonhardt, "Electron-beam produced plasmas: Considerations and applications," *Vac. Technol. Coating*, pp. 24–28, Nov. 2001.

[6] D. Leonhardt, C. Muratore, S. G. Walton, D. D. Blackwell, R. F. Fernsler, and R. A. Meger, "Generation of electron-beam produced plasmas and applications to surface modification," *Surf. Coat. Technol.*, vol. 178, pp. 682–687, 2004.

[7] C. Muratore, D. Leonhardt, S. G. Walton, D. D. Blackwell, R. F. Fernsler, and R. A. Meger, "Low temperature nitriding of stainless steel in an electron beam generated plasma," *Surf. Coat. Technol.*, vol. 191-192, pp. 255–262, 2005.

[8] C. Muratore, S. G. Walton, D. Leonhardt, R. F. Fernsler, D. D. Blackwell, and R. A. Meger, "Effect of plasma flux composition on the nitriding rate of stainless steel," *J. Vac. Sci. Technol. A, Vac. Surf. Films*, vol. 22, pp. 1530–1535, Jul./Aug. 2004.

[9] E. M. Mount II, Ed., "AIMCAL procedure for qualitatively determining metal adhesion," in *Association of Industrial Metallizers, Coaters and Laminators (AIMCAL) Metallizing Technical Reference*, 3rd ed. Fort Mill, SC: Assoc. Ind. Metallizers, Coaters Laminators, 2001. TP-104-87.

[10] D. L. Williamson, O. Ozturk, R. Wei, and P. J. Wilbur, "Metastable phase formation and enhanced diffusion in f.c.c. alloys under high dose, high flux nitrogen implantation at high and low ion energies," *Surf. Coat. Technol.*, vol. 65, pp. 15–23, 1994.

[11] T. Czerwiec, N. Renevier, and H. Michel, "Low-temperature plasma-assisted nitriding," *Surf. Coat. Technol.*, vol. 131, pp. 267–277, 2000.

[12] J. M. Priest, M. J. Baldwin, M. P. Fewell, S. C. Haydon, G. A. Collins, K. T. Short, and J. Tendys, "Low pressure r.f. nitriding of austenitic stainless steel in an industrial-style heat-treatment furnace," *Thin Solid Films*, vol. 345, pp. 113–118, 1999.

[13] E. I. Meletis, "Intensified plasma-assisted processing: Science and engineering," *Surf. Coat. Technol.*, vol. 149, pp. 95–113, 2002.

[14] A. V. Phelps, "The resonant charge exchange cross section of 3.1×10^{-15} cm^{-2}," *J. Phys. Chem. Ref. Data*, vol. 20, pp. 557–573, 1991.

[15] C.-A. Chang, "Enhanced Cu-teflon adhesion by presputtering treatment: Effect of surface morphology changes," *Appl. Phys. Lett.*, vol. 51, pp. 1236–1238, Oct. 1987.

[16] C.-A. Chang, Y.-K. Kim, and S. S. Lee, *Metallized Plastics*, K. L. Mittal, Ed. New York: Marcel Dekker, 1998, pp. 267–291.

[17] D. Youxian, H. J. Griesser, A. W.-H. Mau, R. Schmidt, and J. Liesegang, "Surface modification of poly(tetrafluoroethylene) by gas plasma treatment," *Polymer*, vol. 32, pp. 1126–1130, 1991.

[18] D. J. Wilson, R. C. Pond, and R. L. Williams, "Wettability of chemically modified polymers: Experiment and theory," *Interface Sci.*, vol. 8, pp. 389–399, 2000.

[19] K. Grunke, M. Nitschke, S. Minko, M. Stamm, C. Froeck, F. Simon, S. Uhlmann, K. Pöschel, and M. Motornov, "Merging two concepts: Ultrahydrophobic polymer surfaces and switchable wettability," in *Contact Angle, Wettability and Adhesion*, K. L. Mittal, Ed. New York: Springer-Verlag, 2003, vol. 3, pp. 267–291.

[20] M. A. Lieberman and A. J. Lichtenberg, *Principles of Plasma Discharges and Materials Processing*. New York: Wiley, 1994, pp. 251–256.

[21] D. Leonhardt, S. G. Walton, D. D. Blackwell, D. P. Murphy, R. F. Fernsler, and R. A. Meger, "Ion-ion plasmas from discharges based on electron beam ionization," presented at the 28th IEEE Int. Conf. Pulsed Power Plasma Sci., Las Vegas, NV, Jun. 17–22, 2001.

[22] S. R. Cain, F. D. Egitto, and F. Emmi, "Relation of polymer structure to plasma etching behavior: Role of atomic fluorine," *J. Vac. Sci. Technol. A, Vac. Surf. Films*, vol. 5, pp. 1578–1584, Jul. 1987.

[23] J. M. Grace and L. J. Gerenser, "Plasma treatment of polymers," *J. Dispersion Sci. Technol.*, vol. 24, pp. 305–341, 2003.

[24] D. Gall, S. Kodambaka, M. A. Wall, I. Petrov, and J. E. Greene, "Pathways of atomistic processes on TiN (001) and (111) surfaces during film growth: An *ab initio* study," *J. Appl. Phys.*, vol. 93, pp. 9086–9096, Jun. 2003.

[25] C.-S. Shin, S. Rudenja, D. Gall, N. Hellgren, T.-Y. Lee, I. Petrov, and J. E. Greene, "Growth, surface morphology, and electrical resistivity of fully strained substoichiometric epitaxial $TiN_x (0.67 < x < 1.0)$ layers on MgO (001)," *J. Appl. Phys.*, vol. 95, pp. 356–362, Jan. 2004.

[26] D. D. Blackwell, D. P. Murphy, S. G. Walton, D. Leonhardt, R. F. Fernsler, and R. A. Meger, "Experiments on LAPPS cathode source optimization and development," presented at the 55th Ann. Gaseous Electron. Conf., Minneapolis, MN, 2002.

[27] A. Vizir, V. Gushenets, A. Nikolaev, E. Oks, G. Yushkov, V. Burdovsitin, and N. Rempe, "Recent development and applications of electron, ion and plasma sources based on vacuum arc and low pressure glow," presented at the 31st IEEE Int. Conf. Plasma Sci., Baltimore, MD, Jun./Jul. 2004.

[28] J. D. Jackson, *Classical Electrodynamics*. New York: Wiley, 1967, ch. 13.

[29] S. G. Walton and D. Leonhardt, "Mass Spectral Analysis of Processing Region and the Various Processing Systems have Shown no Anode Material," unpublished.

[30] D. P. Murphy and D. Leonhardt, private communication.

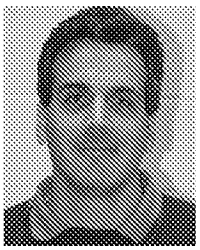

Darrin Leonhardt was born in Brook Park, OH. He received the B.S. degrees in physics and chemistry from Kent State University, Kent, OH, in 1988 and the Ph.D. degree in chemical physics from the University of Maryland, College Park, in 1995.

From 1995 to 1998, he was a National Research Council Postdoctoral Research Fellow in the Chemistry Division at the U.S. Naval Research Laboratory (NRL), Washington, DC. Since 1998, he has been a Research Physicist in the Plasma Physics Division, NRL. Current research interests include plasma modification of materials and surfaces, as well as the fundamental properties of these plasmas.

Dr. Leonhardt is a Member of the American Physical Society and is presently on the Executive Board of American Vacuum Society's Plasma Science and Technology Division.

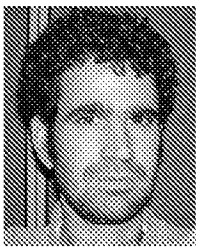

Christopher Muratore was born in New York, NY, on July 8, 1974. He received the B.S. degree in metallurgical and materials engineering and the Ph.D. degree in materials science from the Colorado School of Mines, Golden, in 1999 and 2002, respectively.

He was a Postdoctoral Research Fellow in the Plasma Physics Division at the U.S. Naval Research Laboratory (NRL), Washington, DC, from August 2002 to 2004, where he characterized and used electron beam generated plasmas for nitriding and reactive sputter deposition of materials. He is currently a Visiting Scientist with the Tribology group, U.S. Air Force Research Laboratory, Wright Patterson Air Force Base, Dayton, OH.

Dr. Muratore is a Member of the American Vacuum Society and the Society of Vacuum Coaters.

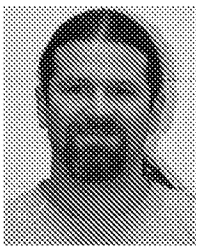

Scott G. Walton was born in Lancaster, PA, on December 23, 1968. He received the B.S. degree in physics from Bloomsburg University of Pennsylvania, Bloomsburg, in 1991 and the M.S. and Ph.D. degrees in physics from The College of William and Mary, Williamsburg, VA, in 1994 and 1998, respectively.

He joined the U.S. Naval Research Laboratory's Plasma Physics Division, Washington, DC, in 1998 as a National Research Council Postdoctoral Research Associate and as a Scientist with SFA, Inc. He became a Research Physicist in the Division, in September, 1992. His research is focused on plasma generation, plasma characterization, and plasma processing, including an interest in new approaches to plasma-based materials modification.

Dr. Walton is Member of the American Vacuum Society and the Society of Vacuum Coaters.